OPEN

Eco-friendly graphene synthesis on Cu foil electroplated by reusing Cu etchants

Ki Chang Kwon[1], Juyoung Ham[2], Sungjun Kim[2], Jong-Lam Lee[2] & Soo Young Kim[1]

[1]School of Chemical Engineering and Materials Science, Chung-Ang University 221 Heukseok-dong, Dongjak-gu, Seoul 156-756, Republic of Korea, [2]Department of Materials Science and Engineering, Pohang University of Science and Technology (POSTECH), Pohang, Gyeongbuk 790-784, Republic of Korea.

Graphene film grown by chemical vapor deposition using Cu substrate is promising for industrial applications. After etching the Cu substrate, which is essential step in graphene transfer process, the etchant solution must be chemically treated to prevent water pollution. Here we investigated that a method of reusing Cu etchant used to synthesize graphene, the synthesis of graphene on the resulting reused Cu films (R-G), and the application of R-G to organic light-emitting diodes (OLEDs) and organic photovoltaic cells (OPVs). The turn-on voltage of OLEDs based on the R-G electrode was 4.2 V, and the efficiencies of OPVs based on the R-G electrode were 5.9–5.95%, that are similar to or better than those of the indium-tin-oxide-based devices. These results suggest that the reusing of Cu foil by the electroplating method could reduce the cost of graphene synthesis, thus opening a wide range of applications in graphene electronics.

Graphene, with sp^2-hybridized hexagonal carbon lattice, has attracted much attention in the electronics field because of its superior mechanical, thermal, optical, and electrical properties[1–3]. Various methods have been reported to synthesize uniform and large-scale graphene sheets, such as exfoliating graphene from graphite using the scotch tape method[4–7]. In particular, graphene film grown by chemical vapor deposition (CVD) is promising for industrial applications because of its large size, high transparency, flexibility, and excellent electrical conductivity[8–10]. Copper, nickel, ruthenium, palladium, and iridium have been reported to be effective metal catalysts for synthesizing CVD graphene sheets[11–14]. Among these metal catalysts, Cu shows the lowest affinity to carbon according to the phase diagram, and thus the carbon solubility in Cu is low, making it very easy to control the graphene thickness[15,16].

To utilize graphene sheets for electronic applications, delamination of graphene from the metal catalyst is essential. Conventional methods of delaminating graphene from a Cu substrate usually includes a chemical etching step, commonly with ferric chloride ($FeCl_3$) or ammonium persulfate [$(NH_4)_2S_2O_8$] solutions[17,18]. After etching the Cu substrate, the etchant solution must be chemically treated to prevent water pollution because of the toxicity of Cu ions to microorganisms or environmental systems[19–21]. Thus, the reusing of Cu ions or Cu foil has become an important issue in the industrial application of graphene. To address this issue, a nondestructive graphene delamination method from Cu foil using an electrochemical reaction was reported[22]. The experimental results showed that the Cu surface became smoother as the step edges and grain boundaries were preferentially etched, and the electrodeposition of Cu nanoparticles filled the trenches and concavities. Furthermore, H_2 bubbling transfer and mechanical delamination transfer of graphene are proposed not to produce etchant solution[23,24].

Electroplating is a process that uses an electrical current to reduce dissolved metal cations so that they form a coherent metal coating on an electrode. Used Cu etchant is always produced in CVD graphene applications. Reusing the Cu etchant as the electrolyte in an electroplating process would make it possible to reuse the Cu foil. This method would reduce the cost of graphene synthesis and prevent water pollution. Furthermore, it is reported that metal films on an oxide layer that is thicker than a certain critical thickness could be more easily detached from the oxide layer owing to the low adhesive force[25,26]. Thus, a Cu film electroplated on an oxide layer could be used in graphene synthesis. Therefore, an investigation of graphene synthesized on electroplated Cu foil is needed.

Here, a method of reusing the Cu etchant used for the synthesis of graphene via an electroplating reaction is demonstrated. Fig. 1 shows the experimental scheme for Cu foil electroplated by reusing Cu etchant. (Further details are available in supplementary Fig. S1) Graphene synthesis on electroplated Cu foil and the application of the synthesized graphene to electronic devices as a transparent electrode are presented. The Cu foil etchant, 1 M
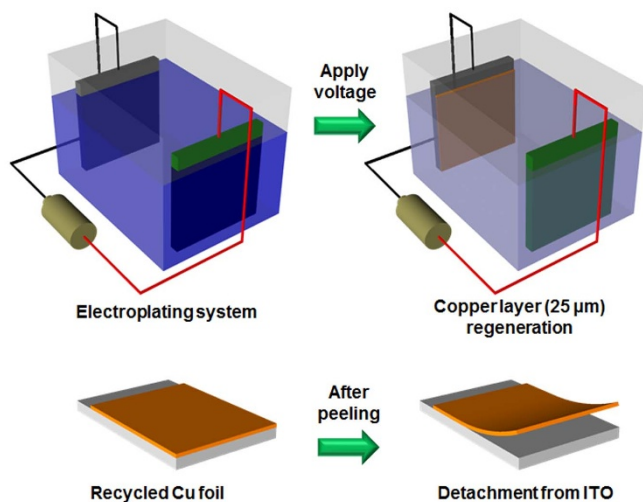
Figure 1 | Schematic illustration of Cu electroplating method. The starting layer was an ITO-coated glass substrate. After substrate completely cleaned, the Cu seed layer (50 nm) was deposited by using thermal evaporator. The Cu sulfate solution collected during the graphene transfer process. After applying the electrical power, the electroplated Cu foil manually detached from the ITO substrate.

$(NH_4)_2S_2O_8$, which is used to facilitate graphene transfer, was reused as the electrolyte in an electroplating reaction that resulted in electroplated Cu foil. Graphene was then synthesized on the electroplated Cu foil. The electroplating reaction and graphene synthesis were performed three times. Field-emission scanning electron microscopy (FE-SEM) and energy dispersive spectrometry (EDS) were used to confirm the surface properties of the as-received (25 μm-thick, Alfa Aesar) and electroplated Cu foils. Atomic force microscopy (AFM) measurements were performed to identify the surface morphology of the electroplated Cu foils. The atomic and molecular structures of all the samples were investigated using the X-ray diffraction (XRD) method. The properties of graphene synthesized on the as-received and electroplated Cu foils were measured by a four-point probe method, UV-visible spectrometry, Raman spectroscopy, transmission electron microscopy (TEM), and X-ray photoemission spectroscopy (XPS). Organic light-emitting diodes (OLEDs) and organic photovoltaic (OPV) cells were fabricated using 4-layer graphene sheets to investigate the effect of Cu etchant reusing on the device performance. Based on these experimental details, the advantages of Cu foil electroplated by reusing Cu etchant are discussed.

Results

Figs. 2a–2d show the FE-SEM and AFM images of the as-received Cu foil and Cu foils electroplated by reusing Cu etchant (R-Cu) at each time [1st R-Cu (etchants from as-received), 2nd R-Cu(etchants from 1st R-Cu), and 3rd R-Cu(etchants from 2nd R-Cu)]. The as-received Cu displayed a very rough surface that included the line-shaped pattern (Further details are available in supplementary Fig. S2). However, the R-Cu foils showed ultra-flat surfaces regardless of electroplating sequence, which indicates that the electroplated Cu foils were uniformly and homogeneously formed. EDS spectra showed no detectable change originating from the electroplating process in the composition. The size of the images was fixed at 2 × 2 μm^2 for the as-received and R-Cu foils. Peak-and-valley shapes, with significant differences in height between the valleys and the peaks, are visible on the surface of the as-received Cu foil. In contrast, all of the R-Cu foils displayed extremely flat surfaces. The root-mean-square (RMS) roughness significantly decreased from 49.1 for the as-received Cu foil to 4.4, 4.8, and 4.5 nm for 1st R-Cu, 2nd R-Cu, and 3rd R-Cu foils,

respectively. It is reported that the surface morphology of the catalytic Cu substrate and the concentration of the carbon feedstock gas are crucial factors in determining the homogeneity and electronic transport properties of graphene products[27–29]. Therefore, it is expected that the use of R-Cu foils could enhance the graphene properties.

Graphene was synthesized on each type of Cu foil using a low-pressure CVD method. To confirm the optical and electrical properties of graphene synthesized on the R-Cu foils, transmittance and sheet resistance were measured and the results are shown in Fig. 3. The sheet resistance slightly decreased from 570 Ω sq^{-1} for the graphene synthesized on the as-received Cu (as-G) foil to 560, 555, and 535 Ω sq^{-1} for the graphene synthesized on the 1st R-Cu (originated from 1st R-G), 2nd R-Cu (originated from 2nd R-G), and 3rd R-Cu (originated from 3rd R-G) foils, respectively. The transmittance values were over 96%, regardless of the sample type, indicating that the transmittance values of graphene were not altered with Cu electroplating. These results indicate that the optical and electrical properties of graphene synthesized on R-Cu foil are competitive with those of graphene synthesized on as-received Cu foil.

Green OLEDs and OPV cells were fabricated to identify the reliability of R-G as an anode. OLED devices with ITO and as-G anodes were also fabricated for comparison (The sheet resistance and work-function of used as electrode sample are available in Supplementary Fig. S3). Figs. 4a and 4b show the current density–voltage and luminance–current density characteristics of OLEDs with different graphene anodes. The device structure is displayed in the inset of fig. 4b. The turn-on voltage of the OLEDs was 4.2 V, regardless of Cu electroplating, which is same as that of the ITO-based device. The leakage current of all the OLEDs—as-G, R-G, and ITO—was the same. The luminance value of OLEDs based on as-G and R-G at a current density of 350 mA/cm^2 was approximately 2.8 × 10^3 cd/m^2, which is comparable to that of the ITO-based OLED. The current density–voltage characteristics of the OPV cells are shown in fig. 4c and the device structure is shown in the inset of fig. 4c. The open-circuit voltage (V_{oc}), short-circuit current (J_{sc}), fill factor (FF), and power conversion efficiency (PCE) of the devices fabricated on as-G are 0.754 V, 13.2 mA/cm^2, 58.6%, and 5.83%, respectively. The PCE values of the R-G devices slightly increased to 5.90–5.95% owing to the increase of the FF. These values are comparable to the values of the ITO-based OPV. Four cells were fabricated simultaneously and the averaged performance values are summarized in Table I. These data suggest that the properties of graphene synthesized on R-Cu foil are similar to or better than those of graphene synthesized on as-received Cu foil.

Discussion

In order to identify the differences between as-received and R-Cu in physical properties, we performed the XRD and XPS measurements. Fig. 5 shows the XRD and XPS analyses of the as-received and R-Cu foils. Three peaks corresponding to Cu(111), Cu(200), and Cu(220) appear in all samples. However, there are significant differences in the peak intensities of the as-received Cu and R-Cu foils. The intensities of Cu(111) and Cu(220) increased and that of Cu(200) decreased in the R-Cu foils as compared with the as-received Cu foil. The intensity of In$_2$O$_3$(222) was dominant in ITO substrate as shown in Supplementary Fig. S4. Therefore the increase of Cu(111) and Cu(220) intensities are thought to come from the crystal structure of ITO. Because Cu has a face-centered cubic structure, the Cu(100), Cu(110), and Cu(111) surfaces have cubic, rectangular, and hexagonal atomic geometries, respectively. The hexagonal lattice structure of graphene is most suitable for the hexagonal Cu(111) facet, suggesting that graphene synthesized on Cu(111) could have ideal properties. In this reasons, the operation time for the synthesis of graphene with the same thickness was reduced from 60 min for the as-received Cu foil to 30 min for the R-Cu foils. It was reported that
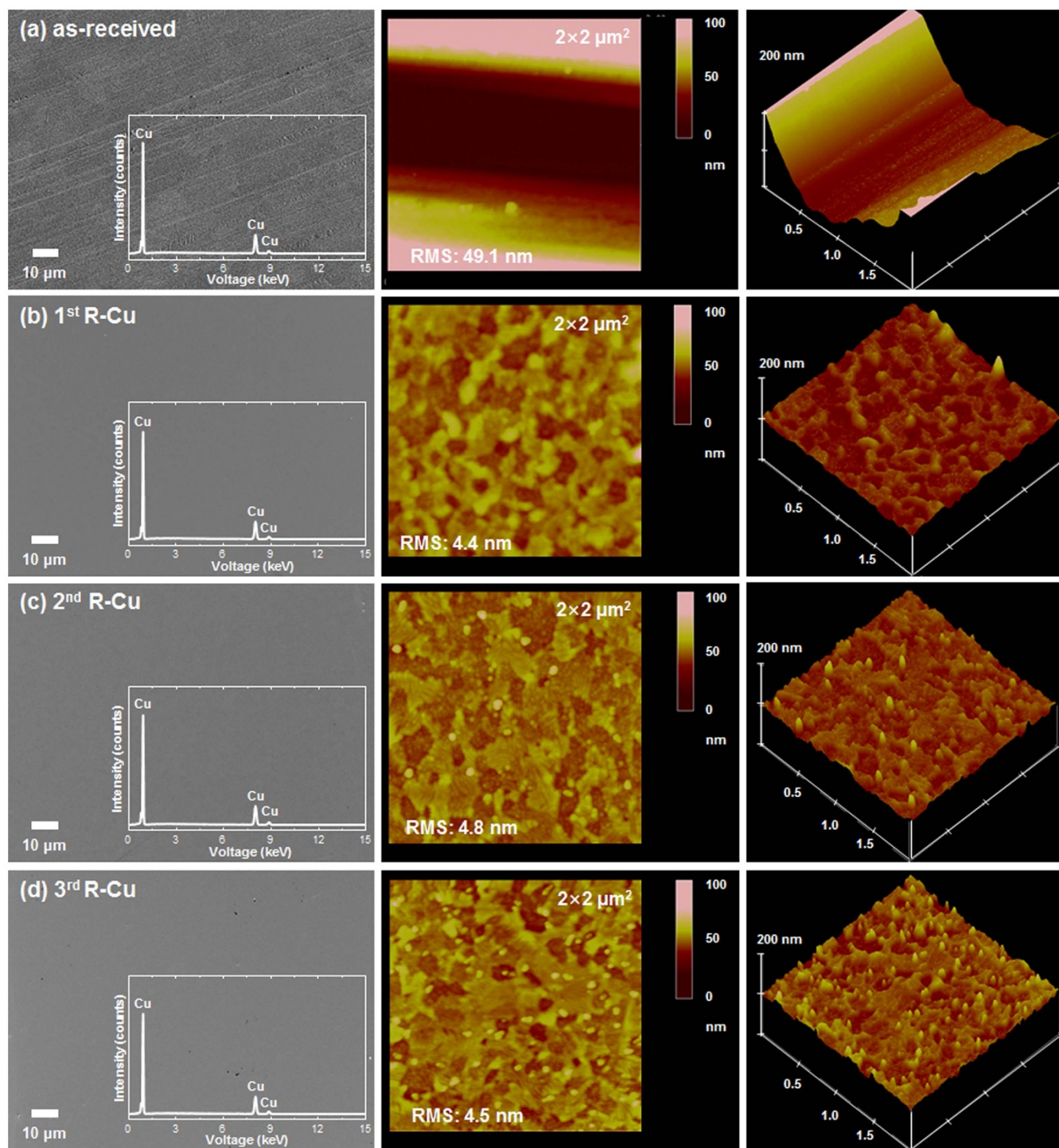
Figure 2 | FE-SEM and AFM images of each different case of Cu foils. (a) as-received, (b) 1st R-Cu, (c) 2nd R-Cu, and (d) 3rd R-Cu foils. Recycled Cu foil shows the smoother surface than as-received ones. The size of images is fixed at 2×2 μm² for as-received and recycled Cu foils. RMS roughness significantly decreased from 49.1 nm to 4.4, 4.8, 4.5 nm for as-received, 1st R-Cu, 2nd R-Cu, and 3rd R-Cu, respectively.

the growth rate of graphene increased linearly as a function of the percentage of (111) facets in the underlying Cu[30,31]. Therefore, it is thought that the large percentage of (111) planes in the R-Cu foils shortened the growth time. Furthermore, the lattice mismatch of graphene with Cu(111), Cu(220), and Cu(200) has been reported to be 3.8, −15.2, and 19.9%, respectively. The mobility of graphene synthesized on the different facets has also been reported to be 2750 [Cu(111)], 2650 [Cu(220)], and 2120 [Cu(200)] cm²/V s[30,31]. Therefore, the increase of the peak intensities in Cu(111) and Cu(220) in the R-Cu foils suggests that the properties of graphene

synthesized on R-Cu foils could be improved. Fig. 5b shows the Cu 2p XPS spectra of the as-received Cu and R-Cu foils (The wide scan of each copper foils is available in Supplementary Fig. S5). No significant difference was found in the samples. It is considered that the electroplating process was strongly related to the crystallographic structure of the Cu foils and did not affect their surface chemistry.

Figs. 6a–6d show the TEM images of as-G, 1st R-G, 2nd R-G, and 3rd R-G. The selected area electron diffraction (SAED) patterns of each sample are shown in the inset of each image. Graphene exhibits a typical wrinkled structure with corrugation and scrolling, which is
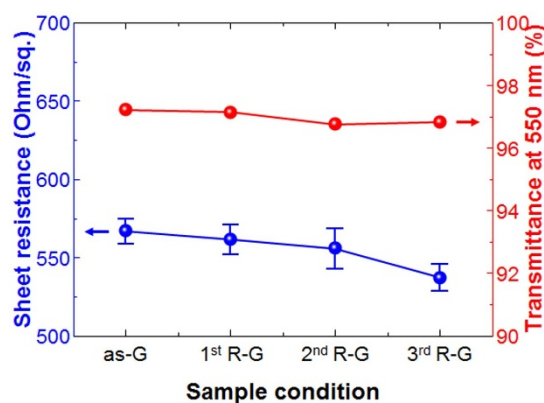
3

Figure 3 | Sheet resistance and transmittance at 550 nm of graphene samples from the each different Cu foils. The sheet resistance and transmittance at 550 nm was slightly decreased in case of graphene from R-Cu foil, regardless of electroplating times, compared to as-received ones. These results show that the optical and electrical properties of R-G were competitive with those of as-received ones.

intrinsic to graphene. Well-defined white diffraction spots are visible in each SAED pattern, regardless of Cu electroplating, confirming the crystalline structure of graphene synthesized on each R-Cu foil. This result suggests that graphene was well synthesized on the R-Cu foils by CVD, even though the growth time of graphene on the R-Cu foils was only half that on the as-received Cu foil. The Raman spectra of graphene synthesized on each Cu foil are displayed in fig. 6e. The G peaks of 1st R-G, 2nd R-G, and 3rd R-G appeared at 1588.5, 1589.2, and 1588.5 cm^{-1}, respectively, values that are lower than the G peak of as-G (1590 cm^{-1}). The positions of the 2D peaks in the R-G samples were shifted to a higher wavenumber as compared with that of as-G. It is reported that 2D peak from graphene on Cu(111) shifted to higher wavenumber due to the compressive strain from the overlap of the honeycomb lattice of graphene with the hexagonal structure of the Cu(111) surface. R-G samples were synthesized on Cu(111) dominant foil as shown in fig. 5(a)[32,33]. Therefore, it is considered that the shift of Raman peak comes from the change of Cu crystal orientation after Cu electroplating. Furthermore, no D peak was found in any of the samples, indicating that there are sufficiently tight bonds between the carbon atoms in the graphene networks, with no defects. Considering the SAED patterns and the intensity ratios of 2D peak to G peak, it seems that two layers of graphene were synthesized.

The C 1s spectra for graphene synthesized on the as-received Cu and R-Cu foils are displayed in fig. 7a. The C 1s peak of each graphene sample was separated into four components: a double carbon bond (C=C) at 284.5 eV, a single carbon bond (C–C) at 285.5 eV, a C–O bond at 286.7 eV, and a carbonyl group (C=O) near 289.0 eV[34]. None of the peak positions changed even when graphene was synthesized on the R-Cu foils. A decrease in the number of carbonyl groups and an increase in the number of carbon double bonds (C=C) were found in the R-G samples as compared with the as-G sample. The carbon and oxygen atomic ratio and the carbon peak intensity ratio of the C=C double bond to the single bond (C–C) are displayed in fig. 7b. The ratios of C atoms and C=C bonds increased in the R-G samples. The hexagonal lattice of the Cu(111) plane tends to be more similar to the graphene lattice than other crystal planes from a crystallographic geometry perspective. Furthermore, the Cu(111) crystallographic plane and a relatively high temperature are reported to be beneficial to the nucleation and growth of graphene, whereas with a sufficient C supply, C supersaturation appears to be the predominant mechanism for the formation of graphene, irrespective of the temperature and crystallography[35]. As shown in fig. 5a, the (111) plane is the preferential orientation of the R-Cu foil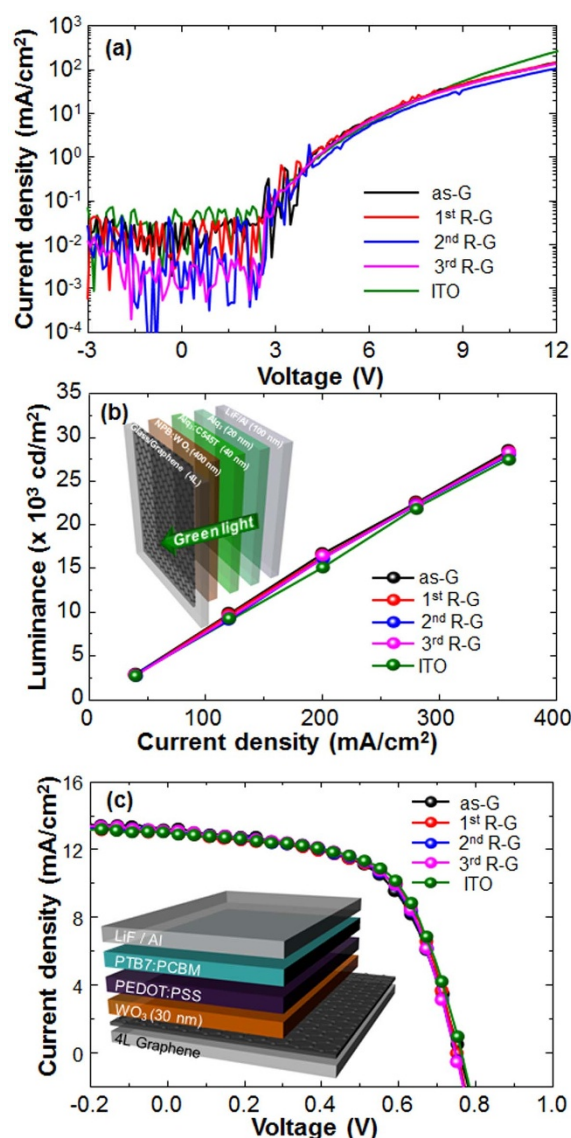s as compared with the as-received Cu foil. Therefore, it is considered that the nucleation barrier of graphene could be reduced

Figure 4 | OLED and OPV device performance was introduced.
(a) Current density–voltage and (b) luminance–current density characteristics of OLEDs with ITO and 4-layer graphene samples. The inset image shows the OLED device structures. The luminance of graphene based samples was slightly higher than ITO based device. (c) Current density–voltage characteristics of OPVs with ITO and graphene samples. The inset image shows the OPV device structures. The efficiency of graphene based device was similar to ITO based ones.

owing to the low lattice mismatch between graphene and the underlying Cu surface, thus increasing the carbon ratio, especially for C=C bonds.

In summary, the properties of graphene synthesized on recycled Cu (R-Cu) foils and the application of the synthesized graphene (R-G) to OLEDs and OPVs as transparent electrodes were investigated. The Cu etchant used in the graphene transfer process was used as the Cu recycling solution. The R-Cu foils were fabricated with an eco-friendly electroplating method. The root-mean-square roughness decreased from 62.3 nm for the as-received Cu foils to 4.3–4.7 nm for the R-Cu foils. The dominant crystal orientation of Cu changed from Cu(200) to Cu(111) and Cu(220). The sheet resistance and transmittance of R-G were 535–560 Ω sq^{-1} and over 96%, respectively, values that are similar to or better than those of as-G. Furthermore, the TEM images, Raman spectra, and XPS data of R-G were

Table 1 | Summary of OPV device results with ITO and graphene samples. The light condition for the measurements was AM 1.5G 100 mW/cm² illumination

OLED electrode		Turn-on voltage (V)	Luminance @ 360 mA/cm² (cd)	OPV electrode		V_{oc} (V)	J_{sc} (mA/cm²)	FF	PCE (%)
ITO		4.5	27468	ITO		0.774	13.0	60.3	6.07
	As-G	4.2	28512		As-G	0.754	13.2	58.6	5.83
Graphene	1st R-G	4.2	28188	Graphene	1st R-G	0.754	13.0	60.2	5.90
	2nd R-G	4.1	27936		2nd R-G	0.754	13.1	60.1	5.94
	3rd R-G	4.15	28044		3rd R-G	0.754	13.1	60.2	5.95

similar to those of as-G. The properties of R-Cu and R-G were similar to those of as-received Cu and as-G, regardless of recycling time. The turn-on voltage of OLEDs based on the R-G electrodes was 4.2 V, and the PCE values of OPVs based on the R-G electrodes were 5.9–5.95%, values that are similar to or better than the values of the as-G-based devices. It is considered that the synthesized graphene structure matches well with the dominant facet of R-Cu(111), resulting in similar or improved device performance. These results suggest that recycling Cu foil by electroplating could reduce the cost of graphene synthesis, thus opening a wide range of applications in graphene electronics.
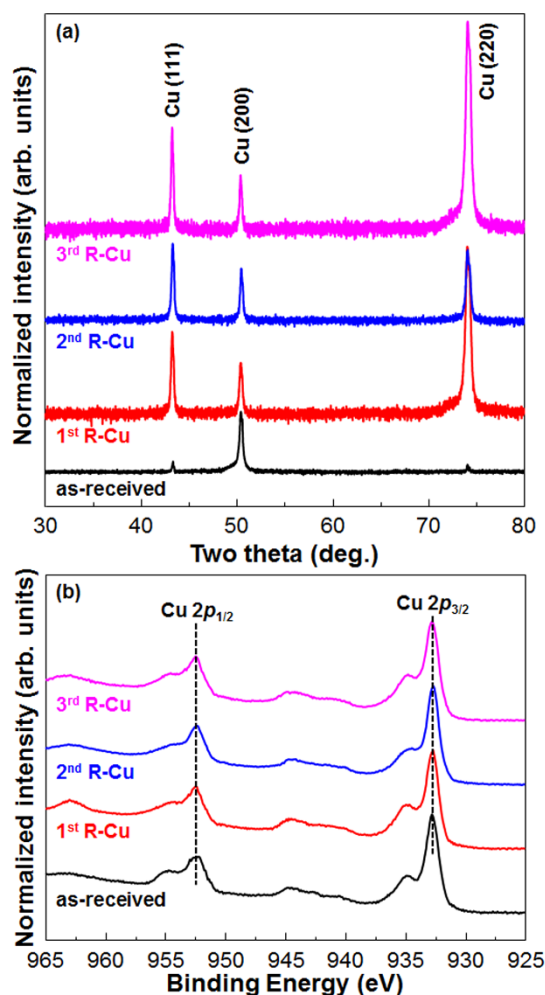

Figure 5 | The XRD and XPS data of each different case of Cu foils. (a) XRD patterns of as-received and recycled Cu foils. The intensity was normalized to Cu(200) facet of as-received Cu foil. The intensity of Cu(111) from recycled Cu foil significantly increased compared to as-received ones. (b) XPS spectra of as-received and recycled Cu foils. The intensity was normalized to Cu $2p_{3/2}$ peak of as-received Cu foil.

Methods

Graphene growth. The as-received and electroplated Cu foils were loaded into a thermal CVD chamber without precleaning. Graphene samples were grown using methane (CH_4) and hydrogen (H_2) gas. Under vacuum conditions of 90 mTorr (12 Pa), the furnace was heated without gas flow for 30 min. Before the growth of graphene, the Cu foil was preheated at 950°C for 30 min. In order to increase the grain size of Cu, H_2 gas was supplied to the furnace under 150 mTorr (20 Pa) of pressure at a rate of 33 cm³/min (sccm). After the preheating step, a gas mixture of CH_4:H_2 = 200:33 sccm was supplied under vacuum conditions for 60 min to synthesize the graphene on the R-Cu foil. The growth time of graphene on the R-Cu foil was reduced to 30 min from 60 min for the as-received Cu foil. After growth, the furnace was cooled to room temperature at a rate of 10–15°C/min under 33 sccm of H_2 flow. Poly(methyl methacrylate) (PMMA) or fluoropolymer (CYTOP) was then spin-coated onto the graphene-coated Cu foil as a supporting material, and the PMMA (or CYTOP)-coated foil was heated on a hot plate to 180°C for 1 min, after which O_2 plasma was used to etch the graphene on the opposite side of the Cu foil. The sample was then immersed in an ammonium persulfate [1M $(NH_4)_2S_2O_8$] bath at room temperature for 3 h to etch away the Cu foil and the etching solution was collected. Then, the remaining PMMA (or CYTOP)-coated graphene was carefully dipped into a de-ionized (DI) water bath 7–9 times to remove any residual etchant. The PMMA (or CYTOP)-coated graphene was then transferred onto a glass substrate. The PMMA (or CYTOP) was removed by an acetone bath at 50°C for 30 min after the PMMA (or CYTOP)/graphene layer had completely adhered to the target substrate.

Electroplating. The starting layer was an ITO-coated glass substrate. The substrate was cleaned with acetone, isopropyl alcohol, and DI water, and then blown dry with nitrogen gas. After the cleaning process, the substrate was put into a thermal evaporation chamber to deposit 50 nm thick Cu as an electroplating seed layer. This substrate was loaded to a cathode holder. The Cu sulfate solution collected during the graphene transfer process was used as the electrolyte for the Cu deposition. During the electroplating process, the current–voltage was measured using a KEITHLEY 2400 source meter. The applied current density (J) was maintained at 15 mA/cm² during the whole process. After electroplating, the sample was rinsed with DI water and the remaining moisture was removed through an annealing process on a hot plate at 100°C. The electroplated Cu substrate was then manually detached from the ITO substrate. The Cu thickness was 25 μm (rate ≈ 16 μm/h @ J = 15 mA/cm²) as measured by a digital micrometer. Graphene synthesis and the electroplating process were repeated three times.

OLED device fabrication. Glass was used as the starting substrate. The substrate was cleaned in sequence with acetone, isopropyl alcohol, and DI water, and then dried with high-purity nitrogen gas. The graphene electrode was transferred onto the glass substrate with CYTOP as a supporting polymer layer to enhance the device performance. The number of graphene layers was fixed at four. The graphene electrodes were treated with HNO_3 and then loaded into the thermal evaporator. WO_3 was doped into a hole transport layer of N,N′-di-[(1-naphthyl)-N,N′-diphenyl]-1,1′-biphenyl-4,4′-diamine (NPB) to reduce the hole injection barrier. The doping concentration of WO3 and thickness of the WO3-doped NPB were fixed at 10 wt% and 400 nm, respectively. Tris(8-hydroxyquinoline) aluminum (Alq_3, 40 nm) doped with fluorescent dye 10-(2-benzothiazolyl)-2,3,6,7-tetrahydro-1,1,7,7-tetramethyl-1H,5H,11H-(1)-benzopyropyrano(6,7-8-i,j)quinolizin-11one (C545T, 1%), undoped Alq_3 (20 nm), LiF (1 nm), and Al (100 nm) layers were deposited in sequence. During deposition, the base pressure of the chamber was maintained at 10^{-6} Torr (800 μPa). The active area of the device was 0.5 × 0.5 mm.

OPV device fabrication. A glass substrate was cleaned in sequence with acetone, isopropyl alcohol, and DI water. After the transfer of the graphene layer with the PMMA supporting layer, the substrate was treated with HNO_3 for 1 h. The substrate was transferred to a thermal evaporation chamber where a WO_3 layer (30 nm) was deposited. A poly(3,4-ethylene- dioxythiophene):poly(styrenesulfonate) (PEDOT:PSS) layer was coated using a bar-coating method that was optimized in advance. These substrates were transferred to a N_2-filled glove box (<0.1 ppm O_2 and H_2O). Poly({4,8-bis[(2-ethylhexyl)oxy]benzo[1,2-b:4,5-b′]dithiophene-2,6-diyl}{3-fluoro-2-[(2-ethylhexyl)carbonyl]thieno[3,4-b]thiophenediyl}) (PTB7, used as received) was first dissolved in 1,2-dichlorobenzene to make a 20 mg/mL solution and then blended with phenyl-C61-butyric acid methyl ester (PCBM, Nano-C, used
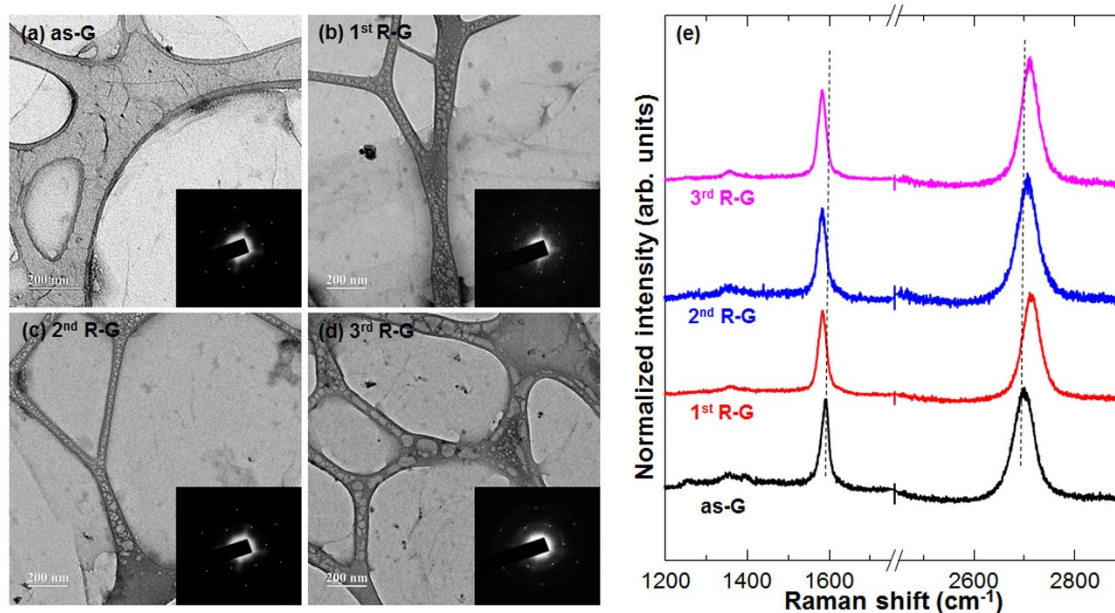
Figure 6 | TEM images of graphene samples from the Cu foils. Graphene was synthesized on (a) as-received, (b) 1st R-Cu, (c) 2nd R-Cu, and (d) 3rd R-Cu foils. The inset images show the crystalline structure of graphene sheet with SAED pattern, regardless of sample type. (e) Raman spectra analysis of the graphene samples.

as received) in a 3 : 2 weight ratio. The thickness of the active layer was measured to be ~200 nm by a surface profiler. The devices were annealed on a hot plate in a glove box at 130°C for 10 min. A cathode consisting of LiF coated with Al was deposited using thermal evaporation. During deposition, the base pressure of the chamber was maintained at 10^{-6} Torr (800 μPa). The active area of the device was 0.5 × 0.5 mm.

Characterization. The sheet resistance was measured in a standard state using a four-point probe method (Keithley 2612A multimeter, USA). UV-visible spectra were recorded on a JASCO V-740 photospectrometer with a wavelength range from 400 to 700 nm. Field-emission SEM (JEOL, JSM-5410LV, Japan) and TEM (JEOL-2100F) images of the as-G and R-G samples were also obtained. Raman spectra of the graphene were obtained with a Lab RAM HR (Horiba Jobin Yvon, Japan) at an

excitation wavelength of 514.54 nm. AFM measurement was performed to identify the surface morphology of the recycled Cu foils. The atomic and molecular structures of all the samples were investigated using XRD. XPS was performed in an ultra-high vacuum chamber [base pressure of $\sim10^{-10}$ Torr (0.133 μPa)] at the 4D beam line equipped with an electron analyzer and heating element in Pohang Acceleration Laboratory. The onset of photoemission corresponding to the vacuum level at the surface of graphene was measured using an incident photon energy of 250 eV with a negative bias on the sample. The results were corrected for charging effects by using Au 4f as an internal reference. The current density–voltage and luminescence–voltage characteristics of the OLEDs and OPVs were measured with a Keithley 2400 semiconductor parameter analyzer under an ambient nitrogen atmosphere (moisture concentration <1 ppm). The photocurrent was measured under AM1.5G 100 mW/
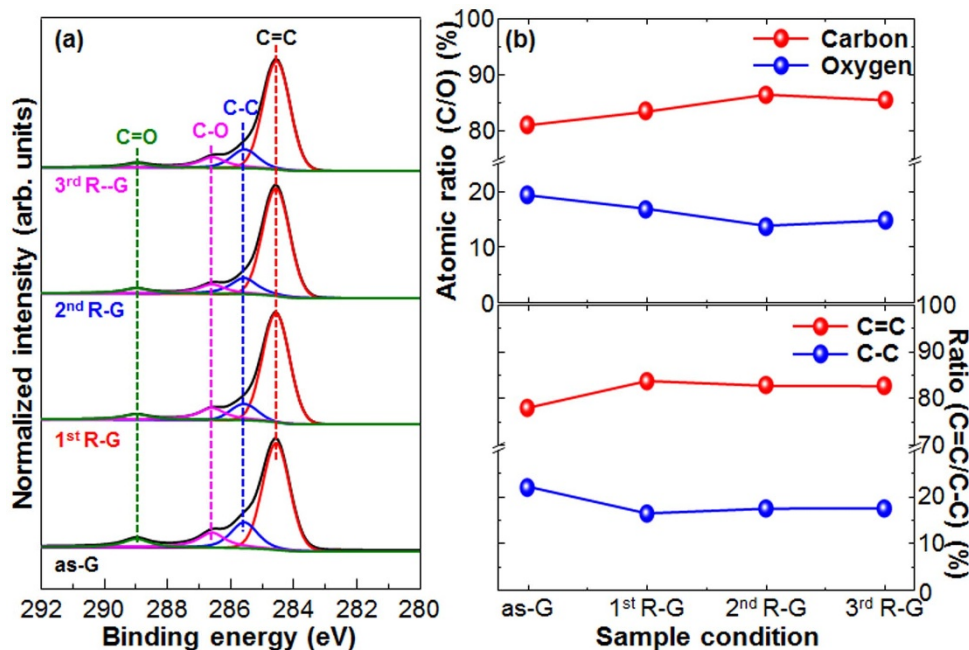

Figure 7 | XPS core level analysis of the graphene samples. (a) C 1s spectra, (b) atomic ratio of carbon to oxygen, and (c) intensity ratio of carbon double bond to single bond. The C=C intensity slightly increased in case of each time recycled Cu foils. The dominant plane, Cu(111), in recycled Cu foil tends to be more similar to graphene lattice than as-receive ones.

cm² illumination from an Oriel 150 W solar simulator. The light intensity was determined using a mono-silicon detector calibrated by the National Renewable Energy Laboratory.

1. Geim, A. K. & Novoselov, K. S. The rise of graphene. *Nat. Mater.* **6**, 183–191 (2007).
2. Meyer, J. C., Geim, A. K., Katsnelson, M. I., Novoselov, K. S., Booth, T. J. & Roth, S. The structure of suspended graphene sheets. *Nature* **446**, 60–63 (2007).
3. Novoselov, K. S. *et al.* Two dimensional gas of massless Dirac fermions in graphenel. *Nature* **438**, 197 (2005).
4. Hernandez, Y. *et al.* High-yield production of graphene by liquid-phase exfoliation of graphene. *Nat. Nanotech.* **3**, 563–568 (2008).
5. Park, S. & Ruoff, R. S. Chemical methods for the production of graphenes. *Nat. Nanotech.* **4**, 217–224 (2009).
6. First, P. N., de Heer, W. A., Seyller, T., Berger, C., Stroscio, J. A. & Moon, J.-S. Epitaxial graphenes on silicon carbide. *MRS Bulletin* **35**, 296–305 (2010).
7. Obraztsov, A. N., Orbraztsova, E. A., Tyurnina, A. V. & Zolutukhin, A. A. Chemical vapor deposition of thin graphene films of nanometer thickness. *Carbon* **45**, 2017–2021 (2007).
8. Bae, S. *et al.* Roll-to-roll production of 30-inch graphene films for transparent electrodes. *Nat. Nanotech.* **5**, 574–578 (2010).
9. Reina, A. *et al.* Large-area, few-layer graphene films on arbitrary substrates by chemical vapor deposition. *Nano Lett.* **9**, 30–35 (2009).
10. Kim, K. S. *et al.* Large-scale pattern growth of graphene films for stretchable transparent electrodes. *Nature* **457**, 706–710 (2009).
11. Kwon, S.-Y. *et al.* & Kodambaka, S. Growth of semiconducting graphene on palladium. *Nano Lett.* **9**, 3985–3990 (2009).
12. Coraux, J. *et al.* Growth of graphene on Ir(111). *New J. Phys.* **11**, 023006 (2009).
13. Li, X. *et al.* Large-area synthesis of high quality and unifrom graphene films on copper films. *Science* **324**, 1312–1314 (2009).
14. Mattevi, C., Kim, H. & Chhowalla, M. A review of chemical vapor deposition of graphene on copper. *J. Mater. Chem.* **21**, 3324–3334 (2011).
15. McLellan, R. The solubility of carbon in solid gold, copper, and silver. *Scr. Metall.* **3**, 389–391 (1969).
16. Lopez, G. A. & Mittemeijer, E. J. The solubility of C in solid Cu. *Scr. Mater.* **51**, 1–5 (2004).
17. Lee, Y. *et al.* Wafer-scale synthesis and transfer of graphene films. *Nano Lett.* **10**, 490–493 (2010).
18. Li, X. *et al.* Transfer of large-area graphene films for high-performance transparent conductive electrodes. *Nano Lett.* **9**, 4359–4363 (2009).
19. Ochoa-Herrera, V., Leon, G., Banihani, Q., Field, J. A. & Sierra-Alvarez, R. Toxicity of copper(II) ions to microorganisms in biological waterwaste treatment systems. *Sci. Total Environ.* **412–413**, 380–385 (2011).
20. Stauber, J. L. & Florence, T. M. Mechanism of toxicity of ionic copper and copper complexes to algae. *Marine Bilolgy* **94**, 511–519 (1987).
21. Jones, R. B. Acute copper and cupric ion toxicity in ans estuarine microbial community. *Appl. Environ. Microb.* **55**, 43–49 (1989).
22. Wang, Y. *et al.* Electrochemical delamination of CVD-grown graphene film: toward the recyclable use of copper catalyst. *ACS nano* **5**, 9927–9933 (2011).
23. Gao, L. *et al.* Repeated growth and bubbling transfer of graphene with millimetre-size single-crystal grains using platinum. *Nat. Comm.* **3**, 1–7 (2012).
24. Yoon, T. *et al.* Direct measurement of adhesion energy of monolayer graphene as-grown on copper and its application to renewable transfer process. Nano Lett. **12**, 1448–1452 (2012).
25. Kim, S. Y., Kim, K., Hong, K. & Lee, J.-L. Investigation of metal peel-off technique for the fabrication of flexible organic light-emitting diodes. *J. Electrochem. Soc.* **156**, J253–J257 (2009).
26. Kim, S. Y., Kim, K., Hong, K. & Lee, J.-L. Flexible organic light-emitting diodes using a metal peel-off method. *IEEE Photonics Technol. Lett.* **20**, 1836–1838 (2008).
27. Benayad, A. *et al.* Controlling work function of reduced graphene oxide with Au-ion concentration. *Chem. Phys. Lett.* **475**, 91–95 (2009).
28. Luo, Z. *et al.* Effect of substrate roughness and feedstock concentration on growth of wafer-scale graphene at atmospheric pressure. *Chem. Mater.* **23**, 1441–1447 (2011).
29. Han, G. H. *et al.* Influence of copper morphology in forming nucleation seeds for graphene growth. *Nano Lett.* **11**, 4144–4148 (2011).
30. Kim, H. *et al.* Activation energy paths for graphene nucleation and growth on Cu. *ACS nano* **6**, 3614–3623 (2012).
31. Shin, H.-J. *et al.* Influence of Cu crystallographic orientation on electron tranport in graphene. *Appl. Phys. Lett.* **102**, 163102 (2012).
32. He, R. *et al.* Large physisorption strain in chemical vapor deposition of graphene on copper substrates. *Nano Lett.* **12**, 2408–2413 (2012).
33. Lee, J.-E., Ahn, G., Shim, J., Lee, Y. S. & Ryu, S. Optical separation of mechanical strain from charge doping in graphene. *Nat. Comm.* **3**, 1024 (2012).
34. Wood, J. D., Schmucker, S. W., Lyons, A. S., Pop, E. & Lyding, J. W. Effect of polycrystalline Cu substrate on graphene growth by chemical vapor deposition. *Nano Lett.* **11**, 4547–4554 (2011).
35. Hu, B., Ago, H., Orofeo, C. M., Ogawa, Y. & Tsuji, M. On the nucleation of garphene by chemical vapor deposition. *New J. Chem.* **36**, 73–77 (2012).

Acknowledgments

Author contributions

K.C.K. performed the synthesized graphene and most of characterization. J.H. and S.K. performed device fabrications. J.-L.L. and S.Y.K. supervised the experiments and contributed to manuscript preparation. J.-L.L. and S.Y.K. initiated and directed the research. S.Y.K. conceived the idea and designed the experiments. All authors were involved in writing the manuscript.

Additional information